On the Calibration of Calorimeter Heat-Transfer Gages

TUDOR SPRINKS*
The University of Southampton, Hampshire, England

Nomenclature

t = time measured after immersion of gage
$q(t)$ = heat transfer to gage
l = gage thickness
ρ = mass density
c = specific heat
α = $(l\rho c)_2$, dynamic-calibration factor of gage
T = temperature
x = space variable
k = coefficient of thermal conductivity
$H(t)$ = unit step function
$A(t)$ = defined by Eq. (5a)
$B(t)$ = defined by Eq. (5b)
$C(t)$ = defined by Eq. (5c)

Subscripts

0 = measured at time $t = 0$
1 = pertaining to the gage
2 = pertaining to the fluid

IN designing a "calorimeter" heat-transfer gage it is required that all incident heat will be absorbed, so that the gage temperature will be raised uniformly. This aim is nearly met if the gage possesses a low specific heat and mass density and a high thermal conductivity, and if the surface of the model on which the gage is mounted has a relatively low thermal conductivity. It is also required that the gage be smoothly mounted and that its presence not affect the aerodynamic heating by being at a temperature significantly different from that of the adjacent model surface. This latter criterion is being considered by the present author in another note.

In practice one endeavors to measure a mean temperature of the gage, as can best be achieved by placing the gauge in a "bridge" circuit. The aerodynamic heating is then assumed to be related to the gage's temperature-time derivative by the linear relation

$$q(t) = (l\rho c)_1(dT_1/dt) \tag{1}$$

$$\equiv \alpha(dT_1/dt), \text{ say} \tag{1a}$$

For maximum accuracy in the use of such a gage, and also to make allowance for the heat lost to the model by conduction from the back and sides of the gage, it is apparent that the dynamic-calibration factor α must be known as accurately as possible. This factor cannot usually be sufficiently well estimated, as not only will the gage be made of an inhomogeneous material possessed of required properties which are indeterminate, but it will also contain such disturbing elements as electric connections and thermocouple insertions.

To find α the author proposes the following technique for calibration. The gage and its backing are first brought to the same uniform air temperature, such as the ambient still-air temperature. The model with its gage (or gages) is then plunged quickly, but smoothly, into a sufficiently large bath of suitable liquid which is initially at a uniform temperature different from that of the model, most conveniently higher than that of the model. The temperature history of the gage is then recorded.

To analyze the behavior of this system it is assumed that the fluid is homogeneous and of two-dimensional semi-infinite extent. At time $t = 0$ the fluid is subjected to the influence of the model's perfect calorimeter gage at the finite boundary of the fluid. The heat-conduction equation for the fluid is

$$\frac{\partial^2 T_2(x,t)}{\partial x^2} = \left(\frac{\rho c}{k}\right)_2 \frac{\partial T_2(x,t)}{\partial t} \tag{2}$$

which we now solve subject to the boundary conditions

$$T_2(x,0) = \text{const} = T_{20} \qquad \text{for } t < 0 \tag{3a}$$

$$T_2(\infty,t) = T_{20} \qquad \text{for all } t \tag{3b}$$

$$T_2(0,t) = T_1(t) \qquad \text{for } t \geqslant 0 \tag{3c}$$

$$q(t) = \alpha \frac{dT_1}{dt} = k_2 \left[\frac{\partial T_2(x,t)}{\partial x}\right]_{x=0} \qquad \text{for } t \geq 0 \tag{3d}$$

Laplace-transform techniques are used to solve for $T_2(x,t)$ and $q(t)$. Finally it is seen that for consistency

$$\frac{q(t)}{T_{20} - T_{10}} = \left[\frac{(k\rho c)_2}{\pi t}\right]^{1/2} - \frac{(k\rho c)_2}{\alpha}\left[\frac{T_{20}H(t) - T_1(t)}{T_{20} - T_{10}}\right] \tag{4a}$$

$$= \alpha \frac{d}{dt}\left[\frac{T_1(t)}{T_{20} - T_{10}}\right] \tag{4b}$$

These two equations now relate the dynamic-calibration factor of the gage α tc its temperature-time history and to the initial temperature of the fluid. We now write

$$\frac{d}{dt}\left[\frac{T_1(t)}{T_{20} - T_{10}}\right] \equiv A(t) \tag{5a}$$

$$\tfrac{1}{2}[(k\rho c)_2/(\pi t)]^{1/2} \equiv B(t) \tag{5b}$$

$$(k\rho c)_2\left\{\frac{T_{20}H(t) - T_1(t)}{T_{20} - T_{10}}\right\} \equiv C(t) \tag{5c}$$

and hence obtain a quadratic equation for α which has the following solutions:

$$\alpha(t) = \left\{\frac{B(t)}{A(t)}\right\}\left[1 \pm \left\{1 - \frac{A(t)\,C(t)}{B^2(t)}\right\}^{1/2}\right] \tag{6}$$

This solution may be evaluated at any time after immersion of the gage. The sign to be chosen in Eq. (6) is that which makes α sensibly constant with time. It is also to be expected that the value of α obtained by the proposed calibration will be not greatly different from an estimated value.

Received by IAS July 26, 1962.
*Research Fellow, Department of Mathematics.

Electrical Properties of Shock Waves on Mars

WILLIAM O. DAVIES*
Armour Research Foundation, Chicago, Ill.

Nomenclature

a = velocity of sound
b = $e^2/3kT$
c = velocity of light
e = electron charge
h = $[3kT/8\pi Ne^2]^{1/2}$ = DeBye length
k = Boltzmann constant
m = electron mass
N = electron number density
n = index of refraction
p = index of absorption
R = radius of curvature of vehicle
T = absolute temperature
t = shock layer thickness

Received by ARS July 30, 1962; revision received October 11, 1962.
* Research Physicist, Physics Division. Member AIAA.

THE electrical properties of the Martian atmosphere at temperatures and densities expected to occur in shock layers for probes circling the planet and the reflection and attenuation by the shock layer of electromagnetic waves having radio and radar frequencies have been calculated. These electrical properties are of interest because of their influence on the propagation of weak fields associated with telemetering signals of deep space communications systems to be used when the Mariner probes explore the Martian atmosphere, and a measurement of electrical properties behind the shock wave also may aid in the evaluation of Martian atmospheric properties.

A model atmosphere for Mars based on presently available astrophysical data estimates the composition to be approximately 98% N_2, with the remaining 2% CO_2 and argon.[1] An isothermal atmosphere is assumed in these calculations, with a temperature of 180°K and a density given by $\rho = \rho_0 \exp(-\beta z)$. It is assumed that the atmosphere is pure nitrogen. Although not sufficiently accurate for some problems (e.g., an accurate determination of spectral radiation characteristics), this assumption can be justified qualitatively for the calculation of electrical properties. Unless a species with a very low ionization potential (e.g., NO) is formed in significant quantities, the results will not be altered greatly. The flight conditions considered are for a probe circling Mars at an altitude of 200,000 ft, with constant velocities of 7200, 10,000, and 15,000 fps (see Table 1).

Electrical properties of the shock layer depend on the a. c. conductivity, which is $\sigma_{a.c.} = (Ne^2/m\nu^2)(1 + \omega^2/\nu^2)^{-1}$. Electron number densities were obtained from equilibrium properties of hot nitrogen.[2] The collision frequency includes encounters of electrons with N_2, N_2^+, N, and N^+. Collision frequencies for neutrals are calculated from kinetic theory. The N_2 cross section was obtained from Massey and Burhop,[3] and the atomic nitrogen cross section is given by Hammerling, Shine, and Kivel.[4] The ion cross sections for singly charged ions, assuming that the interaction is a Coulomb effect,[5] are given by $Q = 8.1b^2 \ln(h/b)$. The a. c. conductivity remains at the d. c. value as long as $\nu \gg \omega$. As the collision frequency and the applied field frequency approach the same magnitude the conductivity decreases, the ω^2 term becomes dominant, and the conductivity decreases rapidly with frequency. The conductivity of the shock waves on Mars is much less than for comparable flight conditions in the earth's atmosphere, a result that could be predicted qualitatively, since the conductivity of hot air is determined largely by the NO concentration.

The two effects of importance are the reflection as the radio wave encounters the discontinuity presented by the shock wave and the attenuation of the signal by absorption as the wave passes through the shock layer. The character and extent of the attenuation and reflection depend on indices of refraction and absorption which are given by

$$n^2, p^2 = \tfrac{1}{2}\{\pm(1 - \sigma_{ac}/\nu\epsilon_0) + [(1 - \sigma_{ac}/\nu\epsilon_0)^2 + (\sigma_{ac}/\omega\epsilon_0)^2]^{1/2}\}$$

The variation of index of refraction with frequency (Fig. 1) reflects the interaction of N, ν, and ω as they influence the conductivity of the gas. At low frequencies the index of refraction varies as $\omega^{-1/2}$; when the conduction current decreases to values comparable to the displacement current, n varies as ω^{-2}; and as the conduction current goes to zero, there is an inflection in the index of refraction. At the highest frequencies, the gas exhibits no response to electric excitation, and the index of refraction approaches unity.

The absorption loss in decibels per meter (Fig. 2) as the wave passes through the ionized gas is given by $\alpha = 8.7\ \omega p/c$. A consideration of this loss requires an estimate of the shock layer thickness which is given[6] approximately by $t = \rho_{12}R$. For a spherical probe 1 m in diameter, the shock layer thickness for velocities of 7200, 10,000, and 15,000 fps are 7, 5, and 3 cm, respectively. From 10^7 to 10^{13} cps, the attenuation is greater than 10 db for Mach 26 shock waves, with a maximum of 1500 db at 10^{11} cps, indicating severe attenuation at all except very high and very low frequencies. For Mach 17 shock waves, the attenuation is also greater than 10 db for 10^{18} to almost 10^{13} cps, whereas for Mach 12 shock waves, the attenuation is much less severe.

Table 1 Shock wave properties on Mars (altitude = 200,000 ft)

Velocity, fps	Mach no. (a = 585 fps)	Flight velocity / Escape velocity	Density, lb/ft³	Temperature, °K
7,200	12	0.42	7.3×10^{-3}	4000
10,000	17	0.60	11.0×10^{-3}	6000
15,000	26	0.88	20.0×10^{-3}	8000

z = altitude
α = absorption loss in decibels per meter
β = scale height = 1.55×10^{-5} ft^{-1}
ϵ_0 = permittivity of free space
ρ_{12} = ratio of atmospheric density to shock layer density
ρ_0 = 0.023 lb/ft³
ν = collision frequency
ω = angular frequency of electromagnetic wave

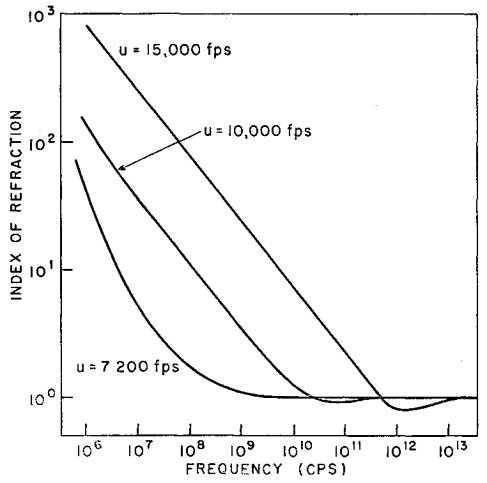

Fig. 1 Index of refraction vs electromagnetic wave frequency. Probe velocity = 7200, 10,000, and 15,000 fps; altitude = 200,000 ft

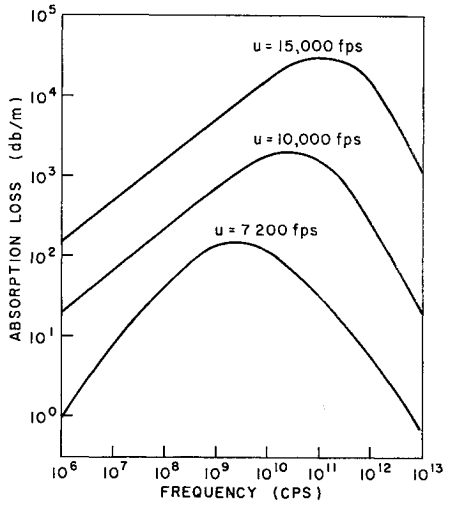

Fig. 2 Absorption loss vs electromagnetic wave frequency. Probe velocity = 7200, 10,000, and 15,000 fps; altitude = 200,000 ft

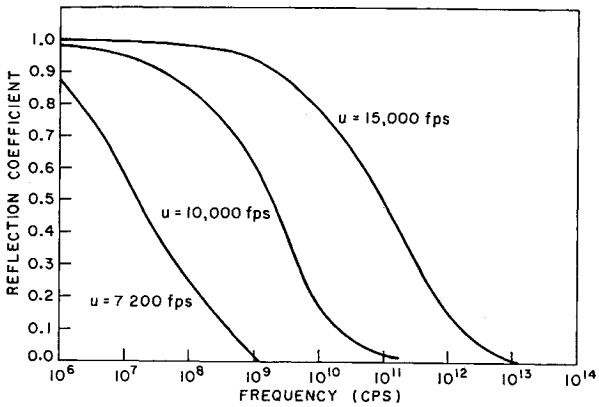

Fig. 3 Reflection coefficient vs electromagnetic wave frequency. Probe velocity = 7200, 10,000, and 15,000 fps; altitude = 200,000 ft

The reflection coefficient calculated for a semi-infinite shock layer, with a plane polarized normally incident em wave, indicates strong reflection for all radio frequencies (Fig. 3). The applicability of this model was examined by calculating the penetration depth to determine if there is sufficient shock layer thickness to establish reflection conditions. At radar frequencies, the penetration depths are the order of millimeters or less, whereas the shock layer thicknesses considered are 3 to 7 cm, indicating that the semi-infinite shock layer model is applicable. For 3-cm radar waves, penetration depths vary from 0.5 mm to 1 cm. At low frequencies the penetration depths are greater than the shock layer thickness considered, and so reflection losses are not predicted accurately by the forementioned model. It appears that low and high frequency signals could be used to transmit information from the probes, although intermediate frequencies (10^8 to 10^{11} cps) would not be available.

References

[1] Kopal, Z., "Aerodynamic effects in planetary atmospheres," Aero-Space Eng. **19**, 10 (1960).

[2] Treanor, C. E. and Logan, J. G., Jr., "Thermodynamics of nitrogen from 2000°K to 8000°K," Cornell Aeronaut. Lab. Rept. BE-1007-A-5 (January 1957).

[3] Massey, H. S. W. and Burhop, E. H. S., *Electronic and Ionic Impact Phenomena* (Oxford Press, New York, 1952), Chap. IV, p. 206.

[4] Hammerling, P., Shine, W. W., and Kivel, B., "Low energy elastic scattering of electrons by oxygen and nitrogen," J. Appl. Phys. **28**, 760 (1957).

[5] Spitzer, L. and Harm, R., "Transport phenomena in a completely ionized gas," Phys. Rev. **89**, 977 (1953).

[6] Meyerott, R. E., *Radiation Heat Transfer to Hypersonic Missiles, Third AGARD Combustion and Propulsion Colloquium* (Pergamon Press, London, 1958), pp. 431–447.

A Vaneless Turbopump

JOSEPH V. FOA*

Rensselaer Polytechnic Institute, Troy, N. Y.

REFERENCE 1 deals with a method of direct energy exchange between flows, consisting of an essentially nondissipative interaction followed by complete mixing at constant pressure. In applications of the method to thrust or lift generation, the final mixing process has no effect on performance if it takes place at ambient pressure. In other situations, however, the effect of mixing on performance is neither negligible nor always beneficial, and there are applications in which it is required that mixing be avoided as much as possible and that the two flows be discharged separately, i.e., before they have mixed appreciably, from the interaction region. Two different ways of effecting this separation are suggested[2] by the observation that the two flows are steady in the relative frame and have different orientations, before they mix, in the stationary frame.

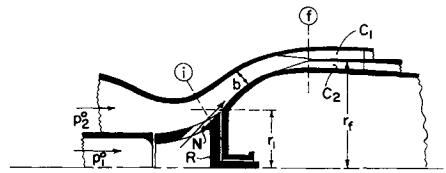

Fig. 1 A vaneless turbopump; R is free-spinning rotor, N a primary discharge nozzle, C_1 and C_2 stationary cascades of separator

This note is a continuation of Ref. 1 and deals specifically with a pumping application in which the two flows leave the interaction region through separate ports before transport processes across their interfaces have made significant progress. Figure 1 illustrates a situation of this type, in which the separation is effected through two stationary cascades C_1 and C_2, one of which is aligned to the primary flow and the other to the secondary flow. The notation will be consistent with that previously employed, and compressibility, viscosity, and heat conduction again will be neglected.

The two flows are extracted from the interaction space at station f, where $p_f = p_e$, $c_{1f}^2 = (1 + \lambda)u_1'^2$, $c_{2f}^2 = (P + \lambda)u_1'^2$, and $V_f^2 = \lambda u_1'^2$. Here, as in Ref. 1,

$$\lambda = \left(1 + \frac{p_e - p_i}{\frac{1}{2}\rho_1 u_1'^2}\right)\left(\frac{r_f}{r_i}\right)^2 \tan\beta_i$$

$$P = \frac{\rho_1}{\rho_2}\frac{1 - (p_e/p_0^0)}{(p_1^0/p_0^0) - (p_e/p_0^0)}$$

From the law of cosines

$$u_{2f}^2 = c_{2f}^2 + V_f^2 - 2c_{2f}V_f \sin\beta_f$$

$$= u_1'^2\left[P + 2\lambda\frac{(1 + \lambda)^{1/2} - (P + \lambda)^{1/2}}{(1 + \lambda)^{1/2} + \mu(P + \lambda)^{1/2}}\right]$$

Since $(p_{2f}^0 - p_e)/(p_1^0 - p_e) = \rho_2 u_{2f}^2/\rho_1 u_1'^2$, it follows that the compression ratio is

$$\frac{p_{2f}^0}{p_0^0} = 1 + 2\lambda\frac{\rho_2}{\rho_1}\frac{(1 + \lambda)^{1/2} - (P + \lambda)^{1/2}}{(1 + \lambda)^{1/2} + \mu(P + \lambda)^{1/2}}\left(\frac{p_1^0 - p_e}{p_0^0}\right)$$

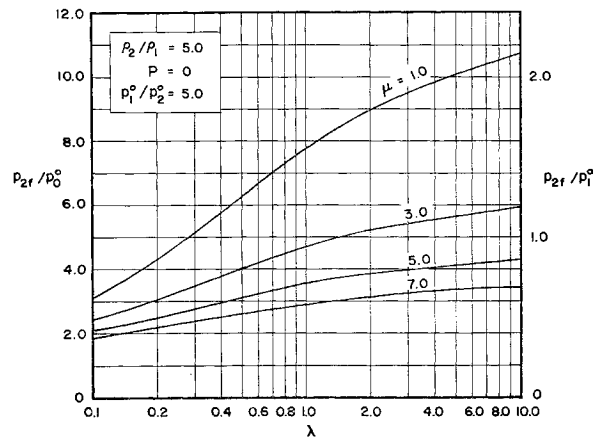

Fig. 2 Ideal compression ratio (with total separation)

Received by ARS August 21, 1962; revision received November 28, 1962. This study was supported by the U. S. Army Transportation Research Command under Grant No. DA TC-44-177-G4.

* Professor of Aeronautical Engineering. Member AIAA.